

# SDGMNet: Statistic-based Dynamic Gradient Modulation for Local Descriptor Learning

Jiayi Ma and Yuxin Deng

**Abstract**—Modifications on triplet loss that rescale the back-propagated gradients of special pairs have made significant progress on local descriptor learning. However, current gradient modulation strategies are mainly static so that they would suffer from changes of training phases or datasets. In this paper, we propose a dynamic gradient modulation, named SDGMNet, to improve triplet loss for local descriptor learning. The core of our method is formulating modulation functions with statistical characteristics which are estimated dynamically. Firstly, we perform deep analysis on back propagation of general triplet-based loss and introduce included angle for distance measure. On this basis, auto-focus modulation is employed to moderate the impact of statistically uncommon individual pairs in stochastic gradient descent optimization; probabilistic margin cuts off the gradients of proportional Siamese pairs that are believed to reach the optimum; power adjustment balances the total weights of negative pairs and positive pairs. Extensive experiments demonstrate that our novel descriptor surpasses previous state-of-the-arts on standard benchmarks including patch verification, matching and retrieval tasks.

**Index Terms**—Local descriptor learning, dynamic gradient modulation, statistical characteristics.

## I. INTRODUCTION

EVALUATING local correspondences of images is a fundamental problem in many computer vision tasks, such as visual localization [32], image registration [22] and retrieval [26]. For this purpose, the classic two-stage pipeline including keypoint detection and patch description was proposed decades ago. Although promising end-to-end methods [54], [5], [30], [42], [20] spring up in recent years, the traditional pipeline remains competitive due to its robustness and efficiency in practice [21]. Moreover, deep local descriptors [10], [38], [2], [44], [56], [11], [14], [19], [51], [55], [45], [48], [6], [43] that are learned with deep neural networks have noticeably outperformed their hand-crafted counterparts, *e.g.*, SIFT [18], and boosted the performance of the two-stage pipeline. Therefore, local descriptors based on deep learning merit deeper study.

Benefiting from the great potentials of Deep Neural Network (DNN), deep local descriptors dispense with heuristic designs to acquire invariance as early efforts [18], [31] did. Overall, local descriptor learning is exactly a branch of metric learning [25]. Specifically, this task aims to encode local patches into discriminative descriptors, and then predict whether pairs of patches are matching or not according to

distances between descriptors. To train the encoder, we need to minimize the distance of matching/positive pairs and maximize non-matching/negative ones in the loss function. Various loss functions taking pairs as basic units are proposed, such as softmax loss with deep metric [10], pair-wise loss [15], triplet loss [2], [23], n-pair loss [44] and ranking loss [11]. Particularly, HardNet [23] constructs a potent triplet loss by mining hard negatives in L2Net [44] batch. Recent works mainly focus on modifying this loss due to its simplicity and superiority.

Besides imposing extra regularization [56], [45] or resampling patches [6], most modifications [14], [51], [55], [48], [43] devote to modulating gradients of pairs according to their hardness of discriminating or identifying. Specifically, if an individual positive pair is too distant to identify, its back-propagated gradients should be weighted more largely during optimization. In contrast, the weight for a hard negative pair that is closer should be larger. Moreover, the hardness of Siamese pairs that share the same anchor also deserves attentions. This kind of hardness can be similarly defined with relative distance. These principles for gradient modulation are so-called hard example mining (HEM). We briefly illustrate them in Fig. 1. HEM also dominates the design of pair-based loss functions in other metric learning tasks [27], [47], [16], [46], [4], [49], [41], [12]. Their successes demonstrate the significance of gradient modulation. However, most modulations are static. The values of the modulation functions depend on individual pairs or Siamese pairs, but do not involve the training phase or the global information. Such modulations suffer from changes of training phases and datasets. Thus, standing on modulating the gradients of individual pairs and Siamese pairs, we concentrate on proposing a dynamic modulation for local descriptor learning. Drawing on global statistical characteristics that are dynamically estimated is promising. Statistics can provide global information that varies over time and datasets, which makes the learning adaptive.

While we are formulating a statistic-based dynamic gradient modulation, more details should be explored. Firstly, related works [43], [57] indicate that once a specific metric, *e.g.*,  $L_2$  distance or inner product is chosen, an implicit modulation harbored in deep back propagation would disorder the elaborate schedule. Secondly, strict HEM should not be encouraged. Because this task is often featured with open-set [7], few-shot [50] and large-scale [17]. For example, the training set of *Liberty* in UBC PhotoTour [52] contains 161K classes with only less than 3 patches in a class on average. It is unreasonable and impossible to fit the hard pairs perfectly. Finally, the balance between the total modulation weights of negative pairs and positive pairs is fatal for optimization. An overwhelmed

This work was supported by the National Natural Science Foundation of China under Grant no. 61773295.

The authors are with the Electronic Information School, Wuhan University, Wuhan, 430072, China (e-mail: jyima2010@gmail.com, dyx\_acuo@whu.edu.cn).

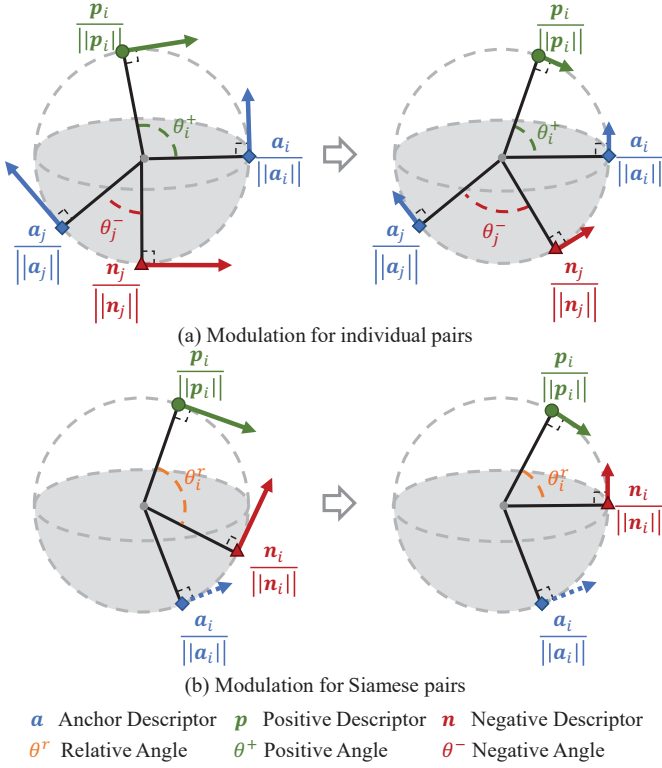


Fig. 1. Illustration of the necessity of gradient modulation. Arrows denote the gradients of descriptors during training. And subscripts represent the indices in a batch. Angle for a pair is defined in Eqn. (3). Relative angle  $\theta^r$  is equal to  $\theta_i^+ - \theta_j^-$ . (a) The magnitude of the gradient of an individual matching pair  $\{\mathbf{a}, \mathbf{p}\}$  should increase with  $\theta^+$ . In contrast, the one of a non-matching pair  $\{\mathbf{a}, \mathbf{n}\}$  should decrease with  $\theta^-$ . (b) Siamese pairs, *i.e.*, a triplet  $\{\mathbf{a}, \mathbf{p}, \mathbf{n}\}$  in SDGMNet desire a smaller weight, when relative angle  $\theta^r$  is diminishing.

ratio of two total weights caused by the modulation would break down the training. In contrast, an appropriate ratio would help convergence and improve generalization.

In this paper, we propose SDGMNet, a statistic-based dynamic gradient modulation to tackle problems mentioned above. SDGMNet is also based on triplet loss proposed by HardNet. We integrate four modifications in SDGMNet. Firstly, we analyze the back-propagated gradient of triplet loss. We explore that angular distance provides the relative flat-tan magnitude characteristic of gradients before modulation. SDGMNet is easily implemented by pair weighting with the included angle as distance measure (Section III-A). Secondly, we propose auto-focus modulation to modulate gradients for individual pairs. Auto-focus modulation utilizes the statistical characteristics of distances between individual pairs. It does not follow HEM principle. It mines statistically reliable pairs whose distances lay around the location of the distribution to orient the optimization (Section III-B). Thirdly, probabilistic margin employs statistical characteristics of relative distance of Siamese pairs, *i.e.*, triplets. It is applied to cut off the gradients of proportional Siamese pairs that are believed to reach the optimums. Meanwhile, the novel margin draws on hard mining for better convergence (Section III-C). Finally, we adjust the ratio of positive and negative total weights with weight normalization and attenuation coefficient (Section III-D). All statistics are estimated dynamically with rough

Bayesian sequential update [3]. Extensive experiments on standard benchmarks including patch verification, matching, retrieval tasks confirm the superiority of the descriptors learned with SDGMNet.

Our contributions can be summarized as follows:

- 1) We explore the special characteristic of angular distance in back propagation.
- 2) We propose statistics-based auto-focus modulation to moderate the impact of uncommon individual pairs.
- 3) We propose dynamic probabilistic margin to mine Siamese pairs that are hard to discriminate.
- 4) We propose power adjustment to balance total weights of negative and positive pairs for better generalization.

## II. RELATED WORKS

In current years, modulating gradients becomes the shared theme of designing pair-based loss functions in metric learning. Modulation strategies can be categorized into two classes: Modulation for individual pairs and modulation for Siamese pairs. We briefly illustrate these two cases with triplet-based loss as an example in Fig. 1. Our method also stands on them. Thus, we try to absorb related modulation strategies no matter whether they are dynamic or exclusive for triplet loss. For better analyzing these cases in related works, let us represent the general loss as  $\mathcal{L}$ .  $d^+(\mathbf{a}, \mathbf{p})$  denotes the general distance between a matching pair  $\{\mathbf{a}, \mathbf{p}\}$ , and  $d^-(\mathbf{a}, \mathbf{n})$  denotes the one between non-matching  $\{\mathbf{a}, \mathbf{n}\}$ . For convenience, we simplify  $d(\cdot)$  as  $d$ .  $d^+ - d^-$  is usually referred to relative distance, denoted by  $d^r$ .  $\theta$  is an instance for  $d$ . Note that, distance and negative similarity are not distinguished deliberately in this paper.

**Modulation for individual pairs.** Several loss functions, such as Lifted Structure Loss [27], Binomial Deviance Loss [53] and NCA [24], treat individual positive and negative pairs unequally. However, not all of them are aware of that while  $\partial \mathcal{L} / \partial d^+$  should be modulated with an increasing function in terms of  $d^+$ ,  $-\partial \mathcal{L} / \partial d^-$  needs decreasing one, if we follow HEM. For local descriptor learning, Keller *et al.* [14] follow HEM. They modulate  $\partial \mathcal{L} / \partial d_i^+$  and  $-\partial \mathcal{L} / \partial d_i^-$  with functions symmetrical about  $(d_i^+ + d_i^-) / 2$  for each triplet. And then global information is crudely fused by shifting the axis of symmetry. Exp-TL [48] conducts more powerful HEM with exponential loss. The new loss makes  $\partial \mathcal{L} / \partial d^+$  increase and  $-\partial \mathcal{L} / \partial d^-$  decrease exponentially. HyNet [43] observes a hidden modulation in deep back propagation. It substitutes hybrid similarity for common similarity, so the hidden modulation is recast. The new modulation balances the needs of two kinds of pairs. In other tasks, Multi-Simi Loss [49] combines Lifted Structure Loss and Binomial Deviance Loss to satisfy respective demands of  $d^+$  and  $d^-$ . Circle Loss [41] fulfills this purpose with Circle Margin. SFace [57] employs sigmoid functions to mine hard pairs. Meanwhile, SFace also finds that the functions are disturbed in deep back propagation. But this problem is left alone and defended to restrain the noise in datasets, *e.g.*, MS-Celeb-1M [9].

**Modulation for Siamese pairs.** The relative hardness of Siamese pairs should be also taken into account. It provides

more reliable information about the data distribution near the shared anchor. For a triplet, its hardness can be measured by  $d_r$ . Harder triplets with larger  $d_r$  should be emphasized with larger  $\partial\mathcal{L}/\partial d^r$  during stochastic gradient descent. Balntas *et al.* [2] introduce a static hard margin for local descriptor learning. The hard margin modulates  $\partial\mathcal{L}/\partial d^r$  with step function in terms of  $d^r$  and prevents easy triplets from backward propagation. Additionally, quadratic triplet loss in SOSNet [45] and scale-aware negative logarithmic softmax loss introduced by Keller *et al.* [14] polish original triplet loss with ‘soft margin’. Thus,  $\partial\mathcal{L}/\partial d^r$  is modulated by continuous functions that monotonically increase with  $d^r$ . Zhang and Rusinkiewicz [55] further enroll Cumulative Distribution Function (CDF) to formulate a dynamic soft margin. Furthermore, n-pair losses are more popular with other metric learning tasks. In those cases, angular margin [16], [46], [4] cuts off partial easy Siamese pairs and achieves great success. Multi-Simi [49] Loss separates Siamese pairs into independent positive and negative parts. The gradients of positive or negative pairs that share the same anchor are associated to be modulated. In contrast, Circle Loss [41] considers two kinds of Siamese pairs together.

Although not all of modulations discussed above are customized for triplet loss we try to modify, there is still something worthy of consideration. Especially, Zhang and Rusinkiewicz [55] have proposed a dynamic modulation for Siamese pairs with CDF, but it is not considerate. Moreover, the deep analysis on back-propagated gradients performed by HyNet [43] and SFace [57] suggests that the hidden modulation deserves more attentions. Additionally, the SFace points out that the strict HEM might be irrational, which indirectly explains the nature of hybrid similarity in HyNet. Adsorbing these ideas, we concentrate on our concerns and propose SDGMNet.

### III. METHODOLOGY

Since SDGMNet majors in dynamically modulating gradients of pairs in triplet loss, a deep investigation on back-propagated gradients should be conducted. We define  $\mathbf{x}(\Omega)$  and  $\mathbf{y}(\Omega)$  as descriptors before normalization, where we omit the input patch and keep parameters of encoder  $\Omega$  as the only input. To facilitate subsequent analysis, we also discard  $(\Omega)$ .  $\mathbf{a}$ ,  $\mathbf{p}$  and  $\mathbf{n}$  are instances of  $\mathbf{x}$  or  $\mathbf{y}$ . Let  $N$  denote batch size,  $\mathbf{D}$  denote the triplet distance batch  $\{d_1^-, d_2^-, \dots, d_N^-; d_1^+, d_2^+, \dots, d_N^+\}$ . Given a general function  $f(\cdot)$  and a distance batch  $\mathbf{D}$ , the general triplet loss  $\mathcal{L}$  can be represented as

$$\mathcal{L}(\mathbf{D}) = f(d_1^-, d_2^-, \dots, d_N^-; d_1^+, d_2^+, \dots, d_N^+). \quad (1)$$

The back-propagated gradient of the loss *w.r.t.* the parameters of the encoder  $\Omega$  can be computed with chain rule [8] as:

$$\begin{aligned} \frac{\partial \mathcal{L}}{\partial \Omega} = & \sum_{i=1}^N \frac{\partial \mathcal{L}}{\partial d_i^+} \left( \frac{\partial d_i^+}{\partial \mathbf{a}_i} \frac{\partial \mathbf{a}_i}{\partial \Omega} + \frac{\partial d_i^+}{\partial \mathbf{p}_i} \frac{\partial \mathbf{p}_i}{\partial \Omega} \right) + \\ & \sum_{i=1}^N \frac{\partial \mathcal{L}}{\partial d_i^-} \left( \frac{\partial d_i^-}{\partial \mathbf{a}_i} \frac{\partial \mathbf{a}_i}{\partial \Omega} + \frac{\partial d_i^-}{\partial \mathbf{n}_i} \frac{\partial \mathbf{n}_i}{\partial \Omega} \right), \end{aligned} \quad (2)$$

where  $(\mathbf{D})$  is omitted. In Eqn. (2),  $\partial\mathcal{L}/\partial d$  is a scalar. It reveals how much the corresponding pair contributes to update of

parameters. Gradient modulation for pairs focuses on rescaling  $\partial\mathcal{L}/\partial d$  with a function about  $d$ . In this way, stochastic gradient descent optimization can be better controlled. However, related works [57], [43] explore that the term  $\partial d/\partial \mathbf{x}$  harbors a hidden modulation function about  $d$  which would break our intention.

#### A. Angular Distance

Consider the term  $\partial d/\partial \mathbf{x}$ . Due to normalization, descriptors are embedded onto unit hypersphere. Included angular  $\theta$  can be used for distance measure. It is defined as

$$\theta = \arccos \frac{\mathbf{x} \mathbf{y}}{\|\mathbf{x}\| \|\mathbf{y}\|}, \quad (3)$$

where  $\|\cdot\|$  denotes  $L_2$  normalization. There are two more common metrics for distance measure: inner product  $s$  and  $L_2$  distance  $l$ . They are defined as

$$s = \frac{\mathbf{x} \mathbf{y}}{\|\mathbf{x}\| \|\mathbf{y}\|}, \quad l = \left\| \frac{\mathbf{x}}{\|\mathbf{x}\|} - \frac{\mathbf{y}}{\|\mathbf{y}\|} \right\|. \quad (4)$$

They are equivalent instances of  $d$  in forward propagation but distinguishing in back propagation. In back propagation,  $\partial\theta/\partial \mathbf{x}$ ,  $\partial s/\partial \mathbf{x}$  and  $\partial l/\partial \mathbf{x}$  share the same optimal direction which is orthogonal to  $\mathbf{x}$  as illustrated in Fig. 1. However, they own special magnitudes as

$$\left\| \frac{\partial \theta}{\partial \mathbf{x}} \right\| = \frac{1}{\|\mathbf{x}\|}, \quad (5)$$

$$\left\| \frac{\partial s}{\partial \mathbf{x}} \right\| = \frac{1}{\|\mathbf{x}\|} \sqrt{1 - s^2}, \quad (6)$$

$$\left\| \frac{\partial l}{\partial \mathbf{x}} \right\| = \frac{1}{\|\mathbf{x}\|} \frac{\sqrt{4l^2 - l^4}}{2l}. \quad (7)$$

As shown above, an implicit modulation takes effect after a metric is chosen. The magnitude of  $\partial\theta/\partial \mathbf{x}$  depends on  $\|\mathbf{x}\|$  only, which would not disturb the modulation function about  $\theta$  we design later. Thus,  $\theta$  is a suitable choice for our further intention. As for the term  $1/\|\mathbf{x}\|$ , we free it for two reasons. Firstly, Ranjan *et al.* [29] observe that a high-quality picture tends to carry large magnitude of feature in similar practice. According to Eqn. (5), high-quality pictures will receive weaker updates and support the feature space at the latter period of training, which may facilitate the optimization. Moreover,  $\mathbf{a}$ ,  $\mathbf{p}$  and  $\mathbf{n}$  interchange in different batches. So the impact of  $1/\|\mathbf{x}\|$  holds balanced globally.

In short,  $\partial\theta/\partial \mathbf{x}$  owns the optimal direction and a plain magnitude for learning. Thus, we employ  $\theta$  for distance measure in SDGMNet. As a result, we can dedicate to gradient modulation for pairs, *i.e.*, formulating  $\partial\mathcal{L}/\partial d$ . Eqn. (2) can be reformulated with  $\theta$  into

$$\frac{\partial \mathcal{L}}{\partial \Omega} = \sum_{i=1}^N w_i^+ \frac{\partial \theta_i^+}{\partial \Omega} - \sum_{i=1}^N w_i^- \frac{\partial \theta_i^-}{\partial \Omega}, \quad (8)$$

where  $\partial\mathcal{L}/\partial d_i$  is replaced by a weight  $w_i$  for convenience. We decompose  $w_i$  into  $w_s \times w_c$  in SDGMNet.  $w_s$  and  $w_c$  will be introduced in following subsections.

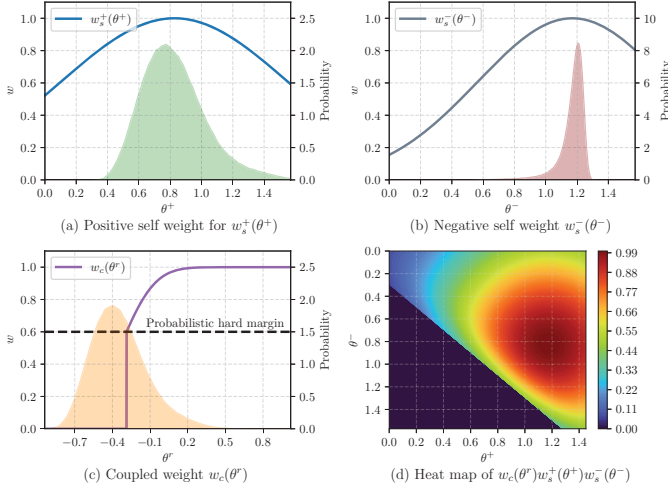


Fig. 2. Visualization of modulation functions and related data distributions at the last training epoch on *Liberty*. Curves in (a), (b) and (c) illustrate three kinds of weights introduced in the text. Shadows demonstrate the probability distribution of variables. (d) is a heat map of  $w_s^+(\theta^+)w_s^-(\theta^-)w_c(\theta^r)$  with  $\theta^+$  and  $\theta^-$  as x-axis and y-axis. The dark red in (d) indicates the strong impact on optimization. Our formulation does not turn the spotlight on hardest triplets that should lay at the top right corner. Easy triplets at the bottom left corner are eliminated by the hard margin.

### B. Auto-focus Modulation

$w_s$  is the weight for modulating the gradients of individual pairs.  $w_s$  is referred to self weight because it is exclusive for a pair.

Ideally, the angular distances of individual negative and the positive pairs reach their own optimums at  $\pi$  and 0, respectively. If following HEM, the gradient of an angle that is further away from its optimum should be weighted more largely. In other words, the gradients of matching pairs should be modulated with  $w_s^+$  that is monotonously increasing w.r.t.  $\theta^+$ , and the non-matching with monotonously decreasing  $w_s^-$ . However, naive distances  $\theta^+$  and  $\theta^-$  are not dependable. Although the hardest positive pairs with large  $\theta^+$  are collected correctly, extreme distortions they carry would damage the convergence of stochastic gradient descent optimization. For the hardest negative pairs of patches, while the real distance between them cannot be evaluated, we simply push their descriptors away. Thus, extreme individual pairs should be treated more cautiously. Successes of HyNet [43] and Sface [57] also imply that excessive HEM on individual pairs should not be advocated.

To neutralize the HEM and extreme individual pairs suppression, we propose auto-focus modulation to formulate dynamic  $w_s^+$  and  $w_s^-$  in SDGMNet as

$$w_s^+(\theta^+) = \exp\left(-\frac{(\theta^+ - E_t[\theta^+])^2}{2(\pi/6 + \text{Std}_t[\theta^+])^2}\right), \quad (9)$$

$$w_s^-(\theta^-) = \exp\left(-\frac{(\theta^- - E_t[\theta^-])^2}{2(\pi/6 + \text{Std}_t[\theta^-])^2}\right), \quad (10)$$

where  $E[\cdot]$  represents the expectation,  $\text{Std}[\cdot]$  denotes the standard deviance, and the subscript  $t$  means the statistical characteristics are dynamically estimated over time. We visualize  $w_s^+(\theta^+)$  and  $w_s^-(\theta^-)$  at the last training iteration in Fig. 2 (a)

and (b). The auto-focus modulation originates from Gaussian blur. It automatically focuses on the expectation of the positive or negative pairs that are more reliable examples we believe. Meanwhile, the impacts of harder and easier examples are weakened. It is worth mentioning that we limit the lower bound of the blur radius to  $\pi/2$ , i.e., add  $\pi/6$  to the standard deviance. If no constraint, the hardest examples that are long-tailed will be cleaned out with extremely small weight. Since the angle of positive pairs and negative pairs spread mainly on  $[0, \pi/2]$  attribute to curse of dimensionality [56], a radius equal to  $3(\pi/6 + \text{Std}_t(\theta))$  is suitable to cover all examples with considerable weights.

### C. Probabilistic Margin

The stochastic gradient descent optimization does not converge until  $\partial\mathcal{L}/\partial\Omega$  approaches zero. Thus, margins are necessary to force  $w$  in Eqn. (8) to be zeros near the optimums. For example,  $\theta_i^+$  holds an ideal optimum at 0, so the  $w_i^+|_{\theta_i^+ < 0+m_i}$  should be 0, where the exclusive margin  $m_i$  can be an infinitesimal. However, it is impossible to search for  $m_i$  for each pair. Furthermore, two margins for matching and non-matching pairs are rational, but a joint margin set for triplets always proves more productive in practice. In other words, a single margin  $m$  designed as a function of  $\theta^r$  is favored. The function modulates Siamese pairs with the same weight. The value of the function couples Siamese pairs, so we name it coupled weight  $w_c$ . How large  $m$  should be set for the global optimum is still confused. Instead of employing a fixed empirical  $m$ , we intend to elaborate a dynamic hard margin that believes  $100 \times m\%$  examples have reached the optimum, so-called probabilistic hard margin.

Given a probabilistic hard margin  $m$ , we learn from the CDF-based soft margin [55] to form  $w_c$  in SDGMNet as

$$w_c(\theta^r) = \begin{cases} \text{CDF}_t(\theta^r), & \theta^r > \text{iCDF}_t(m), \\ 0, & \theta^r \leq \text{iCDF}_t(m), \end{cases} \quad (11)$$

where  $\text{CDF}(\cdot)$  denotes cumulative distribution function,  $\text{iCDF}(\cdot)$  denotes inverse cumulative distribution function. Triplets that carry  $\theta^r$  smaller than  $\text{iCDF}(m)$  are top  $100 \times m\%$  easy examples empirically. These easy examples are believed to approach the optimum and will be isolated from further optimization. The others are preserved and weighted by a monotonously increasing CDF for HEM. HEM for modulating Siamese pairs works well. Due to probabilistic hardness, the modulation is dynamic and adaptive to training data and stage. To facilitate the implementation, we approximate the data distribution with a normal distribution. The curve of  $w_c(\theta^r)$  is drawn in Fig. 2 (c), where we set  $m = 0.6$ . As can be seen, probabilistic hard margin steepens the CDF-based coupled weight to cut off proportional easy triplets.

So far, the coupled weight and self weight in SDGMNet are conceived completely.

### D. Power Adjustment

We define power as the total weight of a class of pairs:

$$P^+ = \sum_{i=1}^N w_i^+, \quad P^- = \sum_{i=1}^N w_i^-. \quad (12)$$



Fig. 3. Network architecture adopted from HyNet [43]. Biases in convolution layers are activated except for the last one. Dropout regularization with 0.3 dropout rate is used before the last convolution layer.

Power describes how strongly a class of positive or negative pairs guides the training with gradients. Before modulation, *i.e.*,  $w = 1$ , the negative power  $P^+$  and the positive power  $P^-$  hold balanced. However, customized modulations on two classes make powers out of control. Intuitively, the positive power guides the model to identify the images with the same label. In contrast, the negative power forces the model to discriminate non-matching examples. An inductive bias on the negative power  $P^-$  would be preferred. Because the model need not identify all labels well which would not appear in the test. Moreover, discriminating ability mutually promotes identifying for human beings. To adjust the ratio of power, we propose weight normalization that divides the weights by the expectation of the corresponding power. Then, attenuation is adopted on the positive side. Finally, SDGMNet is finished as:

$$\frac{\partial \mathcal{L}}{\partial \Omega} = \frac{\alpha}{E_t[P^+]} \sum_{i=1}^N w_i^+ \frac{\partial \theta_i^+}{\partial \Omega} - \frac{1}{E_t[P^-]} \sum_{i=1}^N w_i^- \frac{\partial \theta_i^-}{\partial \Omega}, \quad (13)$$

where  $\alpha$  is the attenuation coefficient.

Without normalization, the scale factor in the previous modulation function would be enabled. Choosing an appropriate scale would be complicated. Moreover, even if a static modulation is employed, the unnormalized power would be still unpredictable due to the varying distribution of data. The ratio of the positive power to the negative power cannot be controlled under such circumstances. Once normalization functions, the ratio of the normalized powers can be quantified and adjusted by the attenuation coefficient. Such a ratio can endure random data, arbitrary modulations and running training phases. Furthermore, the total weight can be regarded as a kind of equivalent learning rate for  $\partial \theta / \partial \Omega$ . Weight normalization guarantees the equivalent learning rate to be stable so that the real learning rate of the optimizer would not be disturbed. As a result, the learning rate can pace as it is proposed to do.

### E. Implementation

**Triplet sampling.** Triplet sampling strategy proposed by HardNet [24] has become the de-facto standard for local descriptor learning. Briefly, HardNet follows L2Net [44] to sample  $N$  matching pairs. For a matching pair, HardNet mines the nearest negative neighbor as the negative example in the triplet. We follow the strategy and employ the anti-noise threshold for hard negative mining. The threshold in angular distance is set to 0.6.

**Network architecture.** L2Net [44] proposes a classic encoder, in which batch normalization [13] and ReLU are

### Algorithm 1 SDGMNet for local descriptor learning

**Input:** SDGMNet hyperparameters  $m$  and  $\alpha$ , vector of initial statistics  $\beta_0$ , raw model, dataset, optimizer.

$t = 1$ ;

**while** training **do**

    Sample a data batch from datasets;

    Compute the angular distance matrix;

    Obtain HardNet triplets;

    Compute statistics  $\mu_t$  in batch, except for the expectation of powers;

    Update corresponding statistics by Eqn. (14);

    Compute  $w_s^+(\theta^+)$ ,  $w_s^-(\theta^-)$  and  $w_c(\theta^r)$  by Eqns. (9), (10) and (11) respectively;

**if** warming **then**

        Set  $w_s^+(\theta^+)$ ,  $w_s^-(\theta^-)$  and  $w_c(\theta^r)$  to 1

**end if**

    Compute powers  $P^+$  and  $P^-$  by Eqn. (12);

    Update the expectation of powers by Eqn. (14);

    Construct pseudo loss by Eqn. (15);

    Call back propagation of pseudo loss;

    Update the model with the optimizer;

$t = t + 1$ ;

**end while**

**Output:** Well-trained model.

employed after each convolution layer except for the last one. HyNet [43] replaces these normalization layers to learnable Filter Response Normalization (FRN) and TLU [39]. Moreover, it introduces an additional normalization layer at the input of the encoder. These modifications remarkably improve local deep descriptor learning with little cost. We adopt this network architecture and illustrate it in Fig. 3.

**Statistics estimation.** There are some statistical arguments varying over time in SDGMNet, which make the modulation dynamic. We employ rough Bayesian sequential update [3] to estimate these arguments as:

$$\beta_t = 0.999\beta_{t-1} + 0.001\mu_t, \quad (14)$$

where  $\beta_t$  is the vector of approximated global statistics and  $\mu_t$  is the estimation in batch at  $t$ th iteration. The past data provide a priori to current training. A fixed replacement rate 0.001 is sensitive enough for the former stage and stable for the latter stage of training.

**Pseudo loss.** We avoid an explicit loss that owns the gradient shown in Eqn. (13). Motivated by general pair weighting framework [49], we define pseudo loss as:

$$\mathcal{L}_P = \frac{\alpha}{E_t[P^+]} \sum_{i=1}^N w_i^+ \theta_i^+ - \frac{1}{E_t[P^-]} \sum_{i=1}^N w_i^- \theta_i^-, \quad (15)$$

where  $\alpha$ ,  $w$ ,  $E_t[P^+]$  and  $E_t[P^-]$  are all constant with regard to the model parameter  $\Omega$ . The gradient of pseudo loss is the same as Eqn. (13) so it can be used to exercise the SDGMNet. Pseudo loss holds an ambiguous optimum and does not satisfy the conditions to be a loss. It is a more general tool to guide the training with arbitrary gradient modulation strategies.



TABLE I

PATCH VERIFICATION PERFORMANCE ON UBC PHOTO TOUR. NUMBERS SHOWN ARE FPR@95 THAT ARE LOWER FOR BETTER. THE BEST SCORES ARE HIGHLIGHTED IN BOLD. DASH LINES INDICATE CHANGES OF MODELS. HARDNET+FRN DENOTES THE VERSION OF HARDNET TRAINED WITH SDGMNET SETTINGS. LIB: *Liberty*, YOS: *Yosemite*, ND: *Notredame*.

Train	ND	YOS	LIB	YOS	LIB	ND	Mean
Test	LIB		ND		YOS		
SIFT [18]	29.84		22.53		27.29		26.55
TFeat [2]	7.39	10.13	3.06	3.80	8.06	7.24	6.64
L2Net [44]	2.36	4.70	0.72	1.29	2.57	1.17	2.23
HardNet [23]	1.49	2.51	0.53	0.78	1.96	1.84	1.51
CDFDesc [55]	1.21	2.01	0.39	0.68	1.51	1.29	1.38
SOSNet [45]	1.08	2.12	0.34	0.67	1.03	0.95	1.03
HardNet+FRN [23], [43]	1.26	1.76	0.41	0.58	1.16	1.05	1.04
HyNet [43]	0.89	<b>1.37</b>	0.34	0.61	0.88	0.96	0.84
SDGMNet	<b>0.82</b>	1.41	<b>0.30</b>	<b>0.46</b>	<b>0.80</b>	<b>0.76</b>	<b>0.76</b>

TABLE II  
STATISTICS ON *Liberty*

Epoch- $th$	30	70	110	150	190
$E[\theta^r](10^{-1})$	-2.86	-3.13	-3.30	-3.39	-3.43
$Std[\theta^r](10^{-1})$	2.37	2.31	2.25	2.21	2.18
$E[\theta^+](10^{-1})$	8.53	8.39	8.31	8.28	8.26
$Std[\theta^+](10^{-1})$	2.24	2.16	2.11	2.04	2.03
$E[\theta^-]$	1.14	1.15	1.16	1.16	1.17
$Std[\theta^-](10^{-2})$	7.78	7.97	8.09	8.15	8.14
$E[P^+]$	281	280	280	279	279
$E[P^-]$	299	297	295	294	294

TABLE III  
STATISTICS ON *Notredame*

Epoch- $th$	30	70	110	150	190
$E[\theta^r](10^{-1})$	-3.13	-3.40	-3.57	-3.65	-3.69
$Std[\theta^r](10^{-1})$	2.33	2.25	2.20	2.15	2.13
$E[\theta^+](10^{-1})$	8.26	8.14	8.06	8.02	8.01
$Std[\theta^+](10^{-1})$	2.18	2.09	2.01	1.96	1.95
$E[\theta^-]$	1.14	1.15	1.16	1.17	1.17
$Std[\theta^-](10^{-2})$	8.66	8.60	8.60	8.60	8.60
$E[P^+]$	281	281	281	281	281
$E[P^-]$	298	297	295	295	294

**Settings.** We implement SDGMNet in PyTorch [28]. The procedure of SDGMNet is shown in Algorithm 1, where we set  $m = 0.6$  and  $\alpha = 0.9$  for the best performance. The network is trained for 200 epochs (200K iterations) with batch size of 1024 and SGD optimizer. Data augmentation is achieved by random rotation, flipping and cropping [23], [55], [37]. Momentum and weight decay of the optimizer are set to 0.9 and 0.0001, respectively. The learning rate is initialized with 1 and divided by 2 after each 10% of iterations. Moreover, the training is warmed up with  $w = 1$  in the first 10% of iterations. During warming, only  $E[P^+]$  and  $E[P^-]$  function but all statistics are estimated in every iteration. As a result, only the initial values of  $E[P^+]$  and  $E[P^-]$  contribute to the full SDGMNet training. We set them to 10000 so that the equivalent learning rate could act similarly as one cycle learning rate policy [40].

#### IV. EXPERIMENTS

We experiment SDGMNet on three benchmarks: UBC PhotoTourism [52], HPatches [1] and ETH 3D reconstruction [34]. Train settings are shown in Section III-E. The test results are compared with state-of-the-art alternatives including SIFT [18], TFeat [2], L2Net [44], HardNet [23], CDFDesc [55], SOSNet [45] and HyNet [43]. All methods output 128-dimensional descriptors that can be evaluated with  $L_2$  distance. Those learned with DNN are trained with data augmentation. HardNet, CDF and SOSNet enroll the same

network architecture proposed by L2Net, which is deeper than TFeat's. HyNet further upgrades the network with FRN. Not that because L2Net, SOSNet and HyNet are not open source, we just report the results from their published papers. For the rest, we validate their records with released codes.

##### A. UBC PhotoTour

UBC PhotoTour [52] is the most widely used dataset for local descriptor learning. It consists of three subsets *Liberty*, *Yosemite* and *Notredame*. The whole dataset contains more than 1.5M patches and 500K labels. Deep descriptors are trained on one subset and tested on the other two. In the standard protocol, the test aims to verify 100K pairs of patches matching or not. We report the false positive rate at 95% recall (FPR@95) for verification results in Table I. Let A-B represent the result trained on A and then tested on B. Compared with the HyNet, our SDGMNet significantly improves YOS-ND and ND-YOS with large margins of 0.15 and 0.2. Only on YOS-LIB a small gap exists. Finally, we obtain a gain of 0.08 on the mean FPR@95. The improvements are considerable for the saturated performance.

Moreover, since statistics are the cores of our dynamic modulation, we show all statistics on three subsets at several epochs in Tables II, III and IV. As we can see, statistics are different among training phases and datasets. Especially,  $E[\theta^r]$  and  $E[\theta^+]$  vary apparently, which make the major contributions on our dynamic gradient modulation. In contrast,

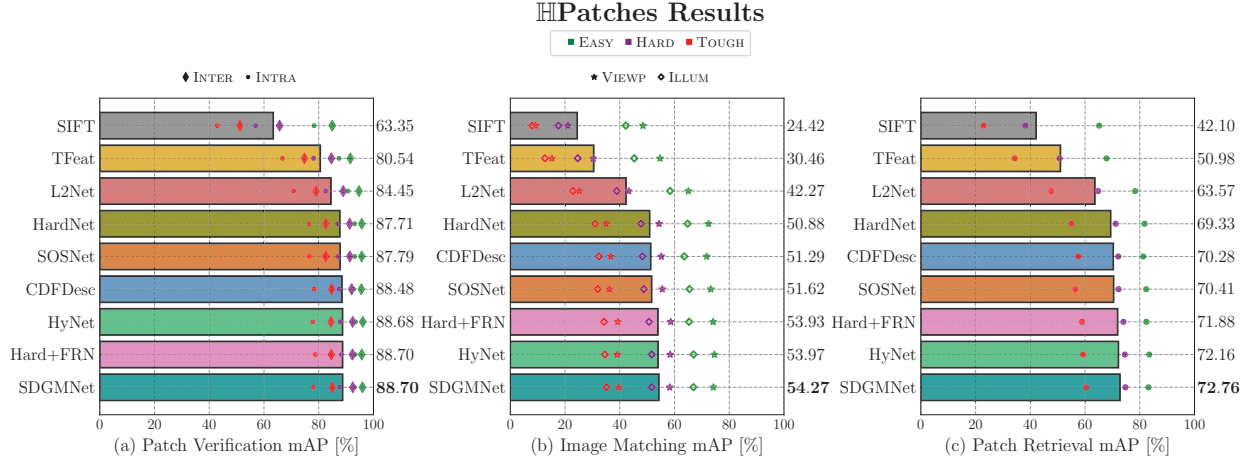


Fig. 4. Test on split ‘a’ of HPatches benchmark. All deep descriptors are trained on *Liberty* of PhotoTour. We report mean average precision (mAP) as evaluation metric. Results of subtasks are marked with different colors and patterns. The bars show the mean scores of subtasks. Mean scores are ranked from lowest to highest.

TABLE IV  
STATISTICS ON *Yosemite*

Epoch- $th$	30	70	110	150	190
$E[\theta^r](10^{-1})$	-3.61	-3.86	-4.00	-4.07	-4.11
$Std[\theta^r](10^{-1})$	2.46	2.41	2.36	2.33	2.31
$E[\theta^+](10^{-1})$	8.10	7.97	7.89	7.85	7.84
$Std[\theta^+](10^{-1})$	2.36	2.30	2.24	2.21	2.19
$E[\theta^-]$	1.17	1.18	1.19	1.19	1.19
$Std[\theta^-](10^{-2})$	6.50	6.65	6.81	6.90	6.97
$E[P^+]$	284	282	280	280	279
$E[P^-]$	304	301	300	298	297

$E[P^+]$  and  $E[P^-]$  keep stable. It suggests that modulation functions change with data distributions dynamically.

### B. HPatches

HPatches [1] is a more comprehensive benchmark that evaluates descriptors on three tasks: patch verification, image matching and patch retrieval. According to geometric distortion, subtasks are categorized into *Easy*, *Hard* and *Tough*. Furthermore, patch pairs from the same or different image sequences are separated into two test subsets for verification, denoted by *Intra* and *Inter*, respectively. And the matching task is designed to evaluate the viewpoint (*VIEWP*) and illumination (*ILLUM*) invariance of descriptors. For a fair comparison, we train SDGMNet on *Liberty* of UBC PhotoTour as other deep descriptors did. Our SDGMNet surpasses predecessors on all three tasks as shown in Fig. 4. In image matching task, while there is no gap between Hard+FRN and HyNet architecture, we improve Hard+FRN with a gain 0.34. In the patch retrieval task, we outperform HyNet with a margin 0.6. The margin is larger than that between SOSNet and CDF whose encoders are the same. In fact, we employ the pre-trained model reported in Table I, which shows the strong generalization of SDGMNet.

However, the evaluation metric, mAP, in standard protocol cannot appropriately reveal the feature matching performance

in practice. Because nearest neighbor matching is the most popular principle for feature matching. Neighbors that are not the nearest make different contributions to the mAP, which run counter to the point of nearest neighbor principle. Thus, we further evaluate SIFT, HardNet and our SDGMNet on raw images of HPatches with nearest neighbor matching. Extreme matching results are shown in Fig. 5. As we can see, although mAP shown in Fig. 4 is considerable, no more than 15% descriptors are correctly matched. Even in some results of SIFT and HardNet, the number of matching pairs is smaller than 4, which is the minimum requirement to evaluate a homography. Our SDGMNet performs relatively well in these extreme conditions. The number of matching pairs significantly mount in our method.

### C. ETH 3D Reconstruction

ETH benchmark [34] also quantifies descriptors on the image matching task. However, it shows more interest in how the matching performance affects the more challenging and practical 3D reconstruction tasks, *i.e.*, structure-from-motion (SFM) and Multi-View Stereo (MVS) [35], [33], [36]. We compare our descriptors with state-of-the-art methods in the standard pipeline of the benchmark. Local patches are extracted by DOG. To directly investigate the performance of descriptors, we abandon the ratio test. All descriptors are trained on *Liberty*. Our pre-trained model reported in Table I is applied here again. The results are shown in Table V. The number of registered images, reconstructed sparse points, dense points demonstrate the completeness of reconstruction. Mean track length is crucial for the reprojection error and reconstruction accuracy. None of descriptors is absolutely outstanding in relatively small subsets. On Madrid Metropolis, we register the largest number of images, which is 19% more than the second place. Compared with other descriptors, our method gets superb scores on all indexes and balances the completeness and accuracy of reconstruction. Also, results on Gendarmenmarkt confirm the superiority of our method for big datasets.

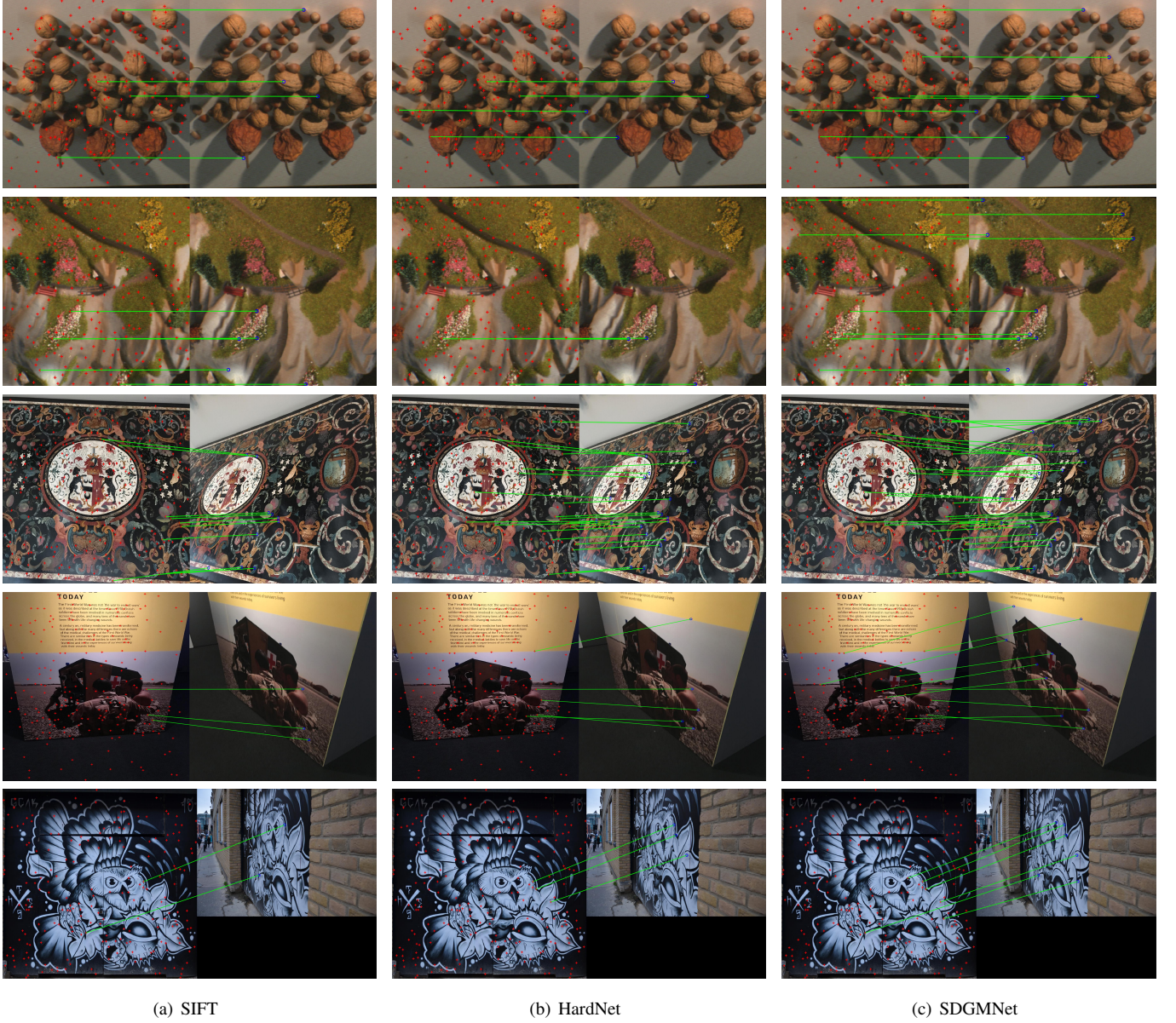


Fig. 5. Feature matching on extreme raw HPatches. The left image of each pair is the reference. The unregistered image is on the right. The first two rows of pairs suffer from illustration variance. The other pairs are pictured from different viewpoints. Obviously, there exists homography between main regions in each image pair. Keypoints are extracted by Difference-of-Gaussians (DOG) detector [18]. 200 keypoints on the reference image are randomly selected and marked with red '+'. All keypoints on the unregistered image are preserved for matching. Descriptors of keypoints are matched by nearest neighbor principle without ratio test. The correctly matched pairs are linked with green lines, while the others are not shown for clarity.

## V. DISCUSSION

### A. Reproducibility

During training on a subset of UBC PhotoTour, we test the model every epoch and report the best core in Table I as several works did. Test results from 101th epoch are shown in Fig. 6 (a). As we can see, the curve of ND easily drops below 0.92, where 0.92 are the state-of-the-art before. To be more rigorous, we have trained the model for 10 times to test the reproducibility. We choose top 10 checkpoints in every training to provide typical values for the records in Table I are  $[0.86 \pm 0.04, 1.55 \pm 0.14, 0.29 \pm 0.02, 0.51 \pm 0.05, 0.88 \pm 0.08, 0.80 \pm 0.06, 0.82 \pm 0.06]$ .

### B. Impact of $m$ and $\alpha$

SDGMNet contains two hyperparameters, namely probabilistic hard margin  $m$  and attenuation coefficient  $\alpha$ . To evaluate the impacts of these two hyperparameters, we train SDGMNet on *Liberty* with one of them changing. Then, we report the average of top 10 checkpoints for higher confidence. The curves of FPR@95 versus  $m$  and  $\alpha$  are drawn in Fig. 6 (b). As shown, a probabilistic hard margin smaller than 0.6 degenerates the performance slightly, which demonstrates that probabilistic hard margin can isolate easy triplets more completely than naive CDF-based soft margin. This modification slightly boosts the descriptors, but an excessively large hard margin would release only a few examples into optimiza-



TABLE V

EVALUATION ON FIVE SUBSETS OF ETH 3D RECONSTRUCTION BENCHMARK. NUMBERS OF UNREGISTERED IMAGES IN DIFFERENT SUBSETS RANGE FROM 8 TO 1463. FIVE CRUCIAL INDEXES FROM THE BENCHMARK ARE SELECTED TO REPORT. THE FIRST AND THE SECOND BEST SCORE ARE MARKED IN RED AND BLUE, RESPECTIVELY.

		#Reg. Images	#Sparse Points	#Dense Points	Track Length	Reproj. Error
Herzjesu (8 images)	HardNet	8	8.7K	239K	4.30	0.50px
	SOSNet	8	8.7K	239K	4.31	0.50px
	HyNet	8	8.9K	246K	4.32	0.52px
	SDGMNet	8	9.0K	233K	4.32	0.53px
Fountain (11 images)	HardNet	11	16.3K	303K	4.91	0.47px
	SOSNet	11	16.3K	306K	4.92	0.46px
	HyNet	11	16.5K	303K	4.93	0.48px
	SDGMNet	11	16.5K	295K	4.94	0.48px
South Building (128 images)	HardNet	128	159K	2.12M	5.18	0.62px
	SOSNet	128	160K	2.12M	5.17	0.63px
	HyNet	128	166K	2.12M	5.14	0.63px
	SDGMNet	128	166K	2.11M	5.16	0.65px
Madrid Metropolis (1334 images)	HardNet	697	261K	1.27M	4.16	0.98px
	SOSNet	675	240K	1.27M	4.40	0.94px
	HyNet	697	337K	1.25M	3.93	0.98px
	SDGMNet	830	278K	1.30M	4.18	0.96px
Gendar- menmarkt (1463 images)	HardNet	1018	827K	2.06M	2.56	1.09px
	SOSNet	1129	729K	3.05M	3.85	0.95px
	HyNet	1181	927K	2.93M	3.49	1.05px
	SDGMNet	1200	763K	3.25M	4.10	1.02px

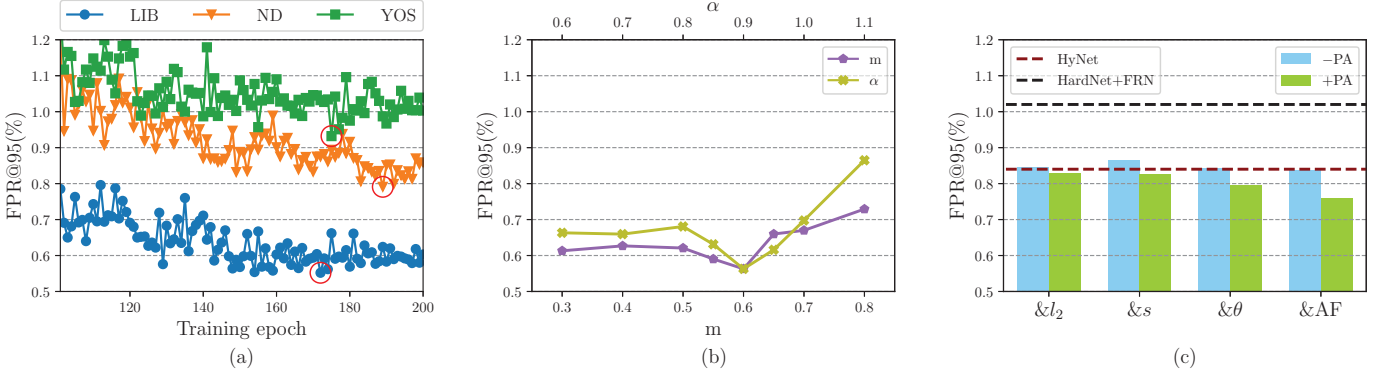


Fig. 6. (a) Checkpoints on different subsets of UBC PhotoTour. Each curve illustrates the mean FPR@95 of two test sets. Marked points are the best scores and the correspondings value are recorded in Table I. (b) Performances on *Liberty* with different probabilistic margin  $m$  or attenuation coefficient  $\alpha$ . The average of top 10 checkpoints are reported (c) Ablation experiments on full UBC PhotoTour. The red and black dashed line denote the mean FPR@95 of HyNet and HardNet+FRN, respectively.

tion, *e.g.*, fewer than 30% with  $m = 0.7$ . Too few examples undoubtedly make the model overfit on current batch and weaken the performance. Compared with  $\alpha$ , varying  $m$  leads to smaller fluctuation. Thus, we do not show the joint impact of two hyperparameters in this paper. We leave the discussion of  $\alpha$  in Section V-D.

### C. Ablation Study

We propose four modifications in SDGMNet, including angular distance, auto-focus modulation (AF), probabilistic margin and power adjustment (PA). In fact, we think of angular distance from the perspective of gradient modulation for individual pairs, which shares the same motivation with AF. In other words, AF and implicit modulations in Eqns. (5), (6) and (7) are kinds of self weight, where the term  $1/\|\mathbf{x}\|$  is

omitted. Let  $\&\theta$ ,  $\&s$ ,  $\&l_2$  denote self weights computed by Eqns. (5), (6), (7), respectively. And  $\&AF$  represents our formulation. We assess frameworks that combine different kinds of self weight with probabilistic-margin-based coupled weight. To test the efficiency of PA, we embed PA to those raw frameworks. Raw frameworks are labeled with -PA and equipped ones with +PA. Related experiments are conducted on full UBC PhotoTour. The performances are shown in Fig. 6 (c).

Without PA, all frameworks outperform the HardNet [24] embedded with FRN (HardNet+FRN). Their scores have been floating near the previous record of HyNet [43]. It is worth mentioning that  $\&l_2$ -PA is equivalent to the HardNet+FRN upgraded with probabilistic margin. Probabilistic margin improves HardNet+FRN by a gain about 0.18. In comparison,

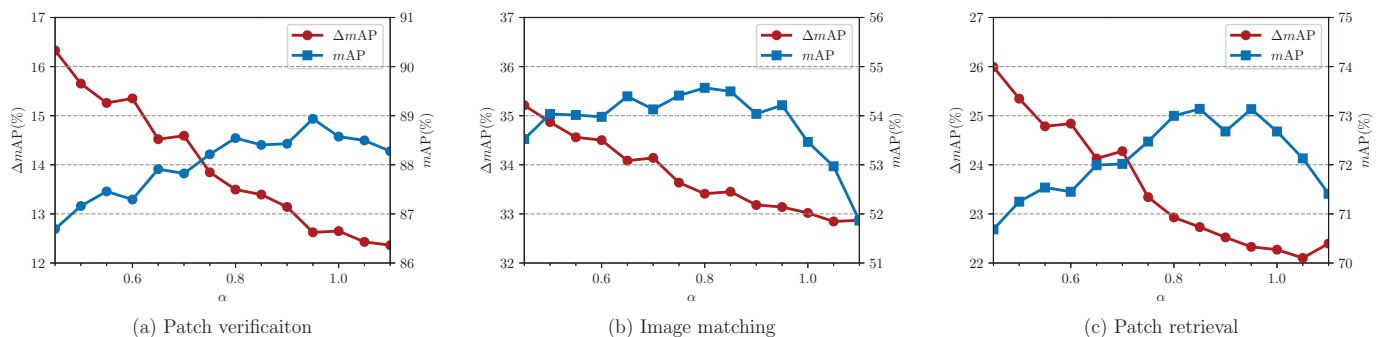


Fig. 7. Impact of  $\alpha$  on HPatches. Models are trained on *Liberty*. Checkpoints at the last epoch are selected to test on HPatches.  $\Delta mAP$  denotes the gap between performances on *Tough* and *Easy*.

a CDF-based soft margin, *i.e.*, CDFDesc [55], improves the HardNet by 0.13 as shown in Table I. While the performance is almost saturated, our novel probabilistic margin still generates a larger improvement. However, angular distance and AF reveal only a little distinction without PA. After PA is equipped, all raw frameworks advance. In such circumstance,  $\&\theta$ +PA and  $\&AF$ +PA show their superiority. Especially,  $\&AF$ +PA builds up a big lead. These outcomes suggest the efficiencies of angular distance, AF and PA.

#### D. Analysis on the Ratio of Powers

Attenuation coefficient  $\alpha$  controls the ratio of the normalized positive power to the negative. The impact of  $\alpha$  shown in Figs. 6 (b) and 7 confirms that an inductive bias to the negative class, *i.e.*, an attenuation coefficient less than 1, is helpful for improvement. Moreover, four raw frameworks (–PA) in Fig. 6 (c) take different modulations, *i.e.*, self weights. They hold mean ratios of powers on three subsets as [1.02, 0.94, 1.00, 0.95]. Better performances emerge when the ratios are forced to 0.9. It means that power adjustments facilitate different modulations. Furthermore, results shown in Fig. 4 are mean scores of full UBC PhotoTour, which imply that the impact of ratio takes effect on various training sets.

To give an insight into how the ratio of power affects the performance, we train the models with different  $\alpha$  on *Liberty* and test them on HPatches. We introduce a naive metric  $\Delta mAP$ , which is computed as  $mAP$  on *Easy* minus  $mAP$  on *Tough*. As shown in Fig. 7, while the  $mAP$  peaks near  $\alpha = 0.9$  in three tasks, the  $\Delta mAP$  tends to decline along with the increasing  $\alpha$ . It can be explained that a ratio small than 1 leads to a preference on the negative part. The model trained with a small ratio cannot learn the extreme variance of positive pairs. It wrongly regards those hard positive pairs as negative ones. Meanwhile, a sizable ratio is enough to help the model handle those easy positive examples. So the performances on easy examples remain relatively stable. In conclusion, the best ratio depends on the difficulty level of the task. Since the difficulty level can be quantified in image matching task, power adjustment for local descriptor learning will be helpful in practice.

## VI. CONCLUSION

In this paper, we propose a statistic-based dynamic gradient modulation for local descriptor learning, called SDGMNet. SDGMNet devotes to dynamically rescaling the gradients of pairs. Firstly, SDGMNet conducts deep analysis on back propagation and chooses included angle for distance measure. The angular distance is unbiased for every pair in theory. Secondly, auto-focus modulation is applied to modulate the gradients of individual pairs. It neutralizes the HEM and extreme example suppression according to statistical characteristics of individual pairs. Thirdly, SDGMNet enrolls statistic-based probabilistic margin to modulate the gradients of Siamese pairs, *i.e.*, triplets. It combines hard and soft HEM on triplets to help stochastic gradient descent optimization converge. Finally, total weights, *i.e.*, powers of two kinds of pairs are adjusted by gradient normalization and attenuation coefficient. SDGMNet fulfills the theme of modulating gradients dynamically with systematical analysis. Local descriptors extracted by SDGMNet show superiority on various tasks and datasets. Every modification in SDGMNet proves efficient by extensive experiments.

Moreover, our success confirms that some extra problems deserve attentions, including hidden modulation in deep back propagation, strict or flexible HEM, balance between powers. Many metric learning tasks, *e.g.*, face recognition share similar frameworks with local descriptor learning. They would suffer from the same problems. Local descriptor learning is a hard task featured with few-shot, open-set and large-scale. Since SDGMNet can systematically tackle those problems for the task, it is promising to transplant solutions of SDGMNet into other metric learning tasks. Moreover, modulating gradient may not lead to a significant improvement as changing a model does. But as a crucial part of optimization for deep learning, it still merits further study.

## REFERENCES

- [1] Vassileios Balntas, Karel Lenc, Andrea Vedaldi, and Krystian Mikolajczyk. Hpatches: A benchmark and evaluation of handcrafted and learned local descriptors. In *CVPR*, pages 5173–5182, 2017.
- [2] Vassileios Balntas, Edgar Riba, Daniel Ponsa, and Krystian Mikolajczyk. Learning local feature descriptors with triplets and shallow convolutional neural networks. In *BMCV*, volume 1, page 3, 2016.
- [3] Christopher M Bishop. *Pattern recognition and machine learning*. springer, 2006.

- [4] Jiankang Deng, Jia Guo, Niannan Xue, and Stefanos Zafeiriou. Arcface: Additive angular margin loss for deep face recognition. In *CVPR*, pages 4690–4699, 2019.
- [5] Daniel DeTone, Tomasz Malisiewicz, and Andrew Rabinovich. Superpoint: Self-supervised interest point detection and description. In *CVPR*, pages 224–236, 2018.
- [6] Patrick Ebel, Anastasiia Mishchuk, Kwang Moo Yi, Pascal Fua, and Eduard Trulls. Beyond cartesian representations for local descriptors. In *ICCV*, pages 253–262, 2019.
- [7] Chuanxing Geng, Sheng-jun Huang, and Songcan Chen. Recent advances in open set recognition: A survey. *PAMI*, 2020.
- [8] Ian Goodfellow, Yoshua Bengio, Aaron Courville, and Yoshua Bengio. *Deep learning*, volume 1. MIT press Cambridge, 2016.
- [9] Yandong Guo, Lei Zhang, Yuxiao Hu, Xiaodong He, and Jianfeng Gao. Ms-celeb-1m: A dataset and benchmark for large-scale face recognition. In *ECCV*, pages 87–102. Springer, 2016.
- [10] Xufeng Han, Thomas Leung, Yangqing Jia, Rahul Sukthankar, and Alexander C Berg. Matchnet: Unifying feature and metric learning for patch-based matching. In *ICCV*, pages 3279–3286, 2015.
- [11] Kun He, Yan Lu, and Stan Sclaroff. Local descriptors optimized for average precision. In *CVPR*, pages 596–605, 2018.
- [12] Yuge Huang, Yuhang Wang, Ying Tai, Xiaoming Liu, Pengcheng Shen, Shaoxin Li, Jilin Li, and Feiyue Huang. Curricularface: adaptive curriculum learning loss for deep face recognition. In *CVPR*, pages 5901–5910, 2020.
- [13] Sergey Ioffe and Christian Szegedy. Batch normalization: Accelerating deep network training by reducing internal covariate shift. In *ICML*, pages 448–456. PMLR, 2015.
- [14] Michel Keller, Zetao Chen, Fabiola Maffra, Patrik Schmuck, and Margarita Chli. Learning deep descriptors with scale-aware triplet networks. In *CVPR*, pages 2762–2770, 2018.
- [15] Vijay Kumar BG, Gustavo Carneiro, and Ian Reid. Learning local image descriptors with deep siamese and triplet convolutional networks by minimising global loss functions. In *CVPR*, pages 5385–5394, 2016.
- [16] Weiyang Liu, Yandong Wen, Zhiding Yu, Ming Li, Bhiksha Raj, and Le Song. Sphreface: Deep hypersphere embedding for face recognition. In *CVPR*, pages 212–220, 2017.
- [17] Ziwei Liu, Zhongqi Miao, Xiaohang Zhan, Jiayun Wang, Boqing Gong, and Stella X Yu. Large-scale long-tailed recognition in an open world. In *CVPR*, pages 2537–2546, 2019.
- [18] David G Lowe. Distinctive image features from scale-invariant keypoints. *International journal of computer vision*, 60(2):91–110, 2004.
- [19] Zixin Luo, Tianwei Shen, Lei Zhou, Siyu Zhu, Runze Zhang, Yao Yao, Tian Fang, and Long Quan. Geodesc: Learning local descriptors by integrating geometry constraints. In *ECCV*, pages 168–183, 2018.
- [20] Zixin Luo, Lei Zhou, Xuyang Bai, Hongkai Chen, Jiahui Zhang, Yao Yao, Shiwei Li, Tian Fang, and Long Quan. Aslfeat: Learning local features of accurate shape and localization. In *CVPR*, pages 6589–6598, 2020.
- [21] Jiayi Ma, Xingyu Jiang, Aoxiang Fan, Junjun Jiang, and Junchi Yan. Image matching from handcrafted to deep features: A survey. *IJCV*, pages 1–57, 2020.
- [22] Jiayi Ma, Ji Zhao, Jinwen Tian, Alan L Yuille, and Zhuowen Tu. Robust point matching via vector field consensus. *TIP*, 23(4):1706–1721, 2014.
- [23] Anastasiya Mishchuk, Dmytro Mishkin, Filip Radenovic, and Jiri Matas. Working hard to know your neighbor’s margins: Local descriptor learning loss. In *NeurIPS*, page 4829–4840, 2017.
- [24] Yair Movshovitz-Attias, Alexander Toshev, Thomas K Leung, Sergey Ioffe, and Saurabh Singh. No fuss distance metric learning using proxies. In *ICCV*, pages 360–368, 2017.
- [25] Kevin Musgrave, Serge Belongie, and Ser-Nam Lim. A metric learning reality check. In *ECCV*, pages 681–699. Springer, 2020.
- [26] Tony Ng, Vassileios Balntas, Yurun Tian, and Krystian Mikolajczyk. Solar: second-order loss and attention for image retrieval. In *ECCV*, pages 253–270. Springer, 2020.
- [27] Hyun Oh Song, Yu Xiang, Stefanie Jegelka, and Silvio Savarese. Deep metric learning via lifted structured feature embedding. In *CVPR*, pages 4004–4012, 2016.
- [28] Adam Paszke, Sam Gross, Francisco Massa, Adam Lerer, James Bradbury, Gregory Chanan, Trevor Killeen, Zeming Lin, Natalia Gimelshein, Luca Antiga, et al. Pytorch: An imperative style, high-performance deep learning library. *arXiv*, 2019.
- [29] Rajeev Ranjan, Carlos D Castillo, and Rama Chellappa. L2-constrained softmax loss for discriminative face verification. *arXiv*, 2017.
- [30] Jerome Revaud, Philippe Weinzaepfel, César De Souza, Noe Pion, Gabriela Csurka, Yohann Cabon, and Martin Humenberger. R2d2: repeatable and reliable detector and descriptor. *arXiv*, 2019.
- [31] Ethan Rublee, Vincent Rabaud, Kurt Konolige, and Gary Bradski. Orb: An efficient alternative to sift or surf. In *ICCV*, pages 2564–2571. Ieee, 2011.
- [32] Torsten Sattler, Will Maddern, Carl Toft, Akihiko Torii, Lars Hammarstrand, Erik Stenborg, Daniel Safari, Masatoshi Okutomi, Marc Pollefeys, Josef Sivic, et al. Benchmarking 6dof outdoor visual localization in changing conditions. In *CVPR*, pages 8601–8610, 2018.
- [33] Johannes L Schonberger and Jan-Michael Frahm. Structure-from-motion revisited. In *CVPR*, pages 4104–4113, 2016.
- [34] Johannes L Schonberger, Hans Hardmeier, Torsten Sattler, and Marc Pollefeys. Comparative evaluation of hand-crafted and learned local features. In *CVPR*, pages 1482–1491, 2017.
- [35] Johannes L Schonberger, Filip Radenovic, Ondrej Chum, and Jan-Michael Frahm. From single image query to detailed 3d reconstruction. In *CVPR*, pages 5126–5134, 2015.
- [36] Johannes L Schönberger, Enliang Zheng, Jan-Michael Frahm, and Marc Pollefeys. Pixelwise view selection for unstructured multi-view stereo. In *ECCV*, pages 501–518. Springer, 2016.
- [37] Connor Shorten and Taghi M Khoshgoftaar. A survey on image data augmentation for deep learning. *JBD*, 6(1):1–48, 2019.
- [38] Edgar Simo-Serra, Eduard Trulls, Luis Ferraz, Iasonas Kokkinos, Pascal Fua, and Francesc Moreno-Noguer. Discriminative learning of deep convolutional feature point descriptors. In *ICCV*, pages 118–126, 2015.
- [39] Saurabh Singh and Shankar Krishnan. Filter response normalization layer: Eliminating batch dependence in the training of deep neural networks. In *CVPR*, pages 11237–11246, 2020.
- [40] Leslie N Smith. Cyclical learning rates for training neural networks. In *WACV*, pages 464–472. IEEE, 2017.
- [41] Yifan Sun, Changmao Cheng, Yuhang Zhang, Chi Zhang, Liang Zheng, Zhongdao Wang, and Yichen Wei. Circle loss: A unified perspective of pair similarity optimization. In *CVPR*, pages 6398–6407, 2020.
- [42] Yurun Tian, Vassileios Balntas, Tony Ng, Axel Barroso-Laguna, Yiannis Demiris, and Krystian Mikolajczyk. D2d: Keypoint extraction with describe to detect approach. In *ACCV*.
- [43] Yurun Tian, Axel Barroso Laguna, Tony Ng, Vassileios Balntas, and Krystian Mikolajczyk. Hynet: Learning local descriptor with hybrid similarity measure and triplet loss. In *NeurIPS*, 2020.
- [44] Yurun Tian, Bin Fan, and Fuchao Wu. L2-net: Deep learning of discriminative patch descriptor in euclidean space. In *CVPR*, pages 661–669, 2017.
- [45] Yurun Tian, Xin Yu, Bin Fan, Fuchao Wu, Huub Heijnen, and Vassileios Balntas. Sosnet: Second order similarity regularization for local descriptor learning. In *CVPR*, pages 11016–11025, 2019.
- [46] Hao Wang, Yitong Wang, Zheng Zhou, Xing Ji, Dihong Gong, Jingchao Zhou, Zhifeng Li, and Wei Liu. Cosface: Large margin cosine loss for deep face recognition. In *CVPR*, pages 5265–5274, 2018.
- [47] Jian Wang, Feng Zhou, Shilei Wen, Xiao Liu, and Yuanqing Lin. Deep metric learning with angular loss. In *ICCV*, pages 2593–2601, 2017.
- [48] Shuang Wang, Yanfeng Li, Xuefeng Liang, Dou Quan, Bowu Yang, Shaowei Wei, and Licheng Jiao. Better and faster: Exponential loss for image patch matching. In *ICCV*, pages 4812–4821, 2019.
- [49] Xun Wang, Xintong Han, Weilin Huang, Dengke Dong, and Matthew R Scott. Multi-similarity loss with general pair weighting for deep metric learning. In *CVPR*, pages 5022–5030, 2019.
- [50] Yaqing Wang, Quanming Yao, James T Kwok, and Lionel M Ni. Generalizing from a few examples: A survey on few-shot learning. *CSUR*, 53(3):1–34, 2020.
- [51] Xing Wei, Yue Zhang, Yihong Gong, and Nanning Zheng. Kernelized subspace pooling for deep local descriptors. In *CVPR*, pages 1867–1875, 2018.
- [52] Simon AJ Winder and Matthew Brown. Learning local image descriptors. In *CVPR*, pages 1–8. IEEE, 2007.
- [53] Dong Yi, Zhen Lei, Shengcai Liao, and Stan Z Li. Deep metric learning for person re-identification. In *CVPR*, pages 34–39. IEEE, 2014.
- [54] Kwang Moo Yi, Eduard Trulls, Vincent Lepetit, and Pascal Fua. Lift: Learned invariant feature transform. In *ECCV*, pages 467–483. Springer, 2016.
- [55] Linguang Zhang and Szymon Rusinkiewicz. Learning local descriptors with a cdf-based dynamic soft margin. In *ICCV*, pages 2969–2978, 2019.
- [56] Xu Zhang, Felix X Yu, Sanjiv Kumar, and Shih-Fu Chang. Learning spread-out local feature descriptors. In *ICCV*, pages 4595–4603, 2017.
- [57] Yaoyao Zhong, Weihong Deng, Jiani Hu, Dongyue Zhao, Xian Li, and Dongchao Wen. Sface: Sigmoid-constrained hypersphere loss for robust face recognition. *TIP*, 30:2587–2598, 2021.